*Acc. Chem. Res.* **2004,** *37,* 269−278

# Ultrasensitive and Quantitative Analyses from Combined Separations−Mass Spectrometry for the Characterization of Proteomes

RICHARD D. SMITH,* YUFENG SHEN, AND KEQI TANG

*Pacific Northwest National Laboratory, P.O. Box 999, Richland, WA 99352*

Received October 1, 2003

**ABSTRACT**

This article describes developments in fundamental and applied aspects of separations, electrospray ionization phenomena, and mass spectrometric instrumentation that are interrelated and important for making more effective and quantitative measurements, particularly for proteomics applications. The basis for better quantitation and ultrahigh sensitivity is highlighted for high-resolution capillary liquid chromatography separations that provide low nanoliter per minute flow rates to an electrospray ionization interface. The increased dynamic range of measurements and low zeptomole regime detection limits obtainable open new avenues for biological research.

## Introduction

Over the past decade, mass spectrometry (MS) has increased its role in biological research due primarily to the development of new biomolecular characterization methods based upon electrospray ionization (ESI)[1] and matrix-assisted laser desorption ionization,[2] ongoing improvements in instrumentation and computer control, and the availability of complete genome sequences. In proteomics, the study of the array of proteins in an organism, tissue, or cell at a given time, MS is becoming the preeminent tool, a role that is unlikely to recede in the foreseeable future.

The need for greater sensitivity in detecting and identifying biomolecules is essentially open-ended; every improvement enables otherwise impractical applications. For example, the ability to make comprehensive proteomic measurements generally depends on the sample size and both the sensitivity and dynamic range of measurements. Improvements in the detection limits (or sensitivity) of measurements can enable qualitatively different approaches involving, for example, the characterization of microdissected cells, microbiopsies, or even single cells. Extending the throughput and range of measurable relative abundances (essentially the dynamic range) can, for example, facilitate the identification of disease specific biomarkers from blood and provide the basis for new clinical assays.

Separations conducted "on-line" with MS allow more complex mixtures to be addressed with greater sensitivity. Combined separations−MS allows species with otherwise unresolvable masses to be distinguished and circumvents the dynamic range limitations inherent for a single mass spectrum. Thus, while the dynamic range achievable in any spectrum constrains the number of detectable species, the use of separations and their effective integration with MS can greatly increase the overall proteomics analysis dynamic range.

Research at our laboratory currently focuses on achieving proteomics and metabolomics measurements of greater sensitivity, dynamic range, and throughput. In this article, we discuss aspects of separations, electrospray phenomena, and MS instrumental developments that are interrelated and important for making more effective and quantitative measurements with an emphasis on application in proteomics.

## Electrospray Ionization Efficiency

A dream for decades was an ionization method that was amenable to biopolymers and that facilitated coupling liquid-phase separations with MS. In the 1980s, Fenn and co-workers showed that ESI-MS enabled analysis of solutions containing thermally labile and nonvolatile compounds, including large proteins.[1]

In ESI, a liquid flowing from a capillary in the presence of a high electric field causes charge separation and, ideally, formation of a stable conical meniscus at the capillary terminus (the ESI emitter).[3] Instabilities in the liquid stream extending from the cone cause breakup into a bimodal distribution of larger (primary) and smaller (satellite) droplets.[4] Less ideal electrosprays result in greater polydispersity.

As droplets shrink by evaporation, asymmetric Coulombic fission occurs as droplet charge approaches the "Rayleigh" limit where electric repulsive forces overcome the liquid surface tension. The fission process is morphologically similar to the initial electrospray droplet formation process,[5] each droplet giving rise to a number of smaller progeny droplets having similar surface charge densities and thus much *larger* charge-to-mass ratios. Both primary and progeny droplets may undergo several fission events, between which they shrink by solvent evaporation. A growing consensus[3,6,7] supports the view that biopolymer ionization is a result of these processes. Larger droplets or more concentrated solutions also yield charged clusters or "residue" particles beyond the $m/z$

Richard D. Smith received his Ph.D. (1975, with Prof. J. H. Futrell) from the University of Utah. He currently holds the positions of Chief Scientist and Battelle Fellow at the Pacific Northwest National Laboratory (PNNL).

Yufeng Shen received his Ph.D. (1998, with Prof. Milton L. Lee) from Brigham Young University. He has been a Senior Research Scientist at PNNL since 2000.

Keqi Tang received his Ph.D. (1994, with Prof. Alessandro Gomez) from Yale University. He held positions at ThermoFinnigan as Research and Development Scientist and YSI Inc. as Senior Mechanical Engineer, before joining PNNL as a Senior Research Scientist in 2000.

* To whom correspondence should be addressed. Phone (509) 376-0723. Fax (509) 376-7722.

10.1021/ar0301330 CCC: $27.50 
Published on Web 02/25/2004

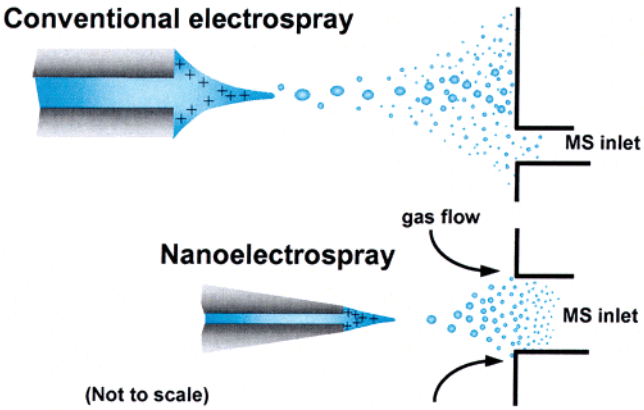


**FIGURE 1.** Normal flow rate electrospray (top) vs a lower flow rate electrospray (bottom) that produces smaller droplets. By allowing closer proximity to the MS inlet, the lower flow rate electrospray affords more efficient ion introduction. See Table 1.

range of most MS. Charged multimeric proteins generally dissociate in a manner analogous to asymmetric droplet fission, yielding a highly charged monomer (at lower $m/z$) and a higher $m/z$ multimeric "residue" (often beyond the range of many spectrometers).[8]

The average number of possible fission events depends on the initial droplet size. Ions are formed more rapidly and efficiently from smaller droplets and with less need for heating. Smaller droplets also move more readily toward the periphery of the electrospray plume due to their smaller inertia and higher charge density[4] (Figure 1, top). Consequently, electrosprays are often sampled "off-axis" (Figure 1 top) or orthogonally by the MS inlet, where the density of desolvated ions is highest and concentrations of large clusters, droplets, or residue particles that can cause contamination or detector noise are minimal.

Two important points emerge regarding the sensitivity of conventional flow rate (approximately microliter per minute) ESI sources. First, a large fraction of the biopolymer analyte can end up as either charged clusters or residue particles depending primarily on flow rate, analyte concentration, and surface activity. Second, due to the ~1 cm spacing between the electrospray emitter and the MS inlet necessary for solvent evaporation, the expansion of the electrospray plume limits inlet efficiency (Figure 1, top). Thus, sensitivity is limited by both ionization and inlet sampling efficiencies.

ESI-MS response typically appears more concentration-sensitive at conventional flow rates than mass-sensitive; that is, increasing flow rate does not generally significantly increase signal.[9] Our first ESI interface for capillary electrophoresis (CE)−MS demonstrated subfemtomole detection limits[10] due to the relatively low CE flow rates. Further studies using a "sheath-flow"-assisted ESI interface showed that higher sensitivity was obtained by employing smaller diameter capillaries, where both the sample size introduced for analysis and the liquid flow rate in the capillary were proportionally reduced.[11] CE−MS using 10 $\mu$m i.d. capillaries[12] at low nanoliter per minute flow rates resulted in mass-sensitive response behavior due to the limited delivery of charge-carrying species. In 1993, we described an ESI source that used an etched conical ESI emitter and sub-microliter-per-minute flow rates to provide improved stability and utility for previously problematic aqueous solutions. The smaller electrospray droplet size allowed "on-axis" emitter alignment and closer proximity to the MS inlet, yielding more efficient ion introduction and increased sensitivity (Figure 1, bottom).[13]

**Table 1. Comparison of Electrospray Characteristics at Conventional and Nano-ESI Flow Rates**

| flow rate | conventional (5 $\mu$L/min) | nano-ESI (20 nL/min) |
|---|---|---|
| droplet diameter[a] | 1.4[b]−6 $\mu$m[c] | 150[c]−220 nm[b] |
| electrospray current[d] | 200 nA | 12 nA |
| droplet generation rate | $7 \times 10^5$ [c] to $6 \times 10^7$ [b] $s^{-1}$ | $6 \times 10^7$ [b] to $2 \times 10^8$ [c] $s^{-1}$ |
| molecules/droplet (1 $\mu$M analyte concentration) | 860[b]−7200[c] | 1[c]−3[b] |
| charges/droplet | $2 \times 10^4$ [b] to $2 \times 10^6$ [c] | 400[c]−1250[b] |
| charges/analyte (1 $\mu$M concentration) | 25[b,c] | 360[b,c] |

[a] Reference 19. [b] Reference 15. [c] Reference 14. [d] Measured.

In 1994, Wilm and Mann[14] described a "nanoelectrospray ionization" (nanoESI) source based upon a capillary with a small emitter orifice diameter that provided a self-limited flow rate of 20−40 nL/min. They showed ionization efficiency increased by ~100-fold compared to conventional ESI flow rates. The extended analyses (up to ~30 min) from microliter sample volumes made nanoESI attractive for many applications.

Both Wilm and Mann[14] and de la Mora and Loscertales[15] developed models that reasonably describe the relationship among flow rate, droplet size, and electrospray current. Table 1 compares the characteristics of electrosprays for both conventional and nanoESI flow rates.

A key point is that at sufficiently low flow rate and concentration, there is on average less than one analyte molecule per droplet. Thus, ionization efficiencies approach 100% since all the analyte is dispersed in very small, easily desolvated, charged droplets. The efficiency of ion transmission through the MS inlet is also optimized. As discussed next, lower flow rate electrosprays also improve quantitation.

## Discrimination, Suppression and Matrix Effects in ESI

Quantitative measurements are facilitated when compound-to-compound response is uniform and varies linearly with concentration. Large variations in ESI-MS response can be observed, often dependent upon other species in solution.[3,16] Reduction or elimination of MS response resulting from the presence of another analyte is referred to as "ion suppression" or a "matrix effect" when caused by another solution component (e.g., buffer).

Quantitation can be problematic at conventional ESI flow rates. A large fraction of a higher concentration analyte is converted to charged residue or clusters (Figure 2, top). The fission process leads to a physical separation

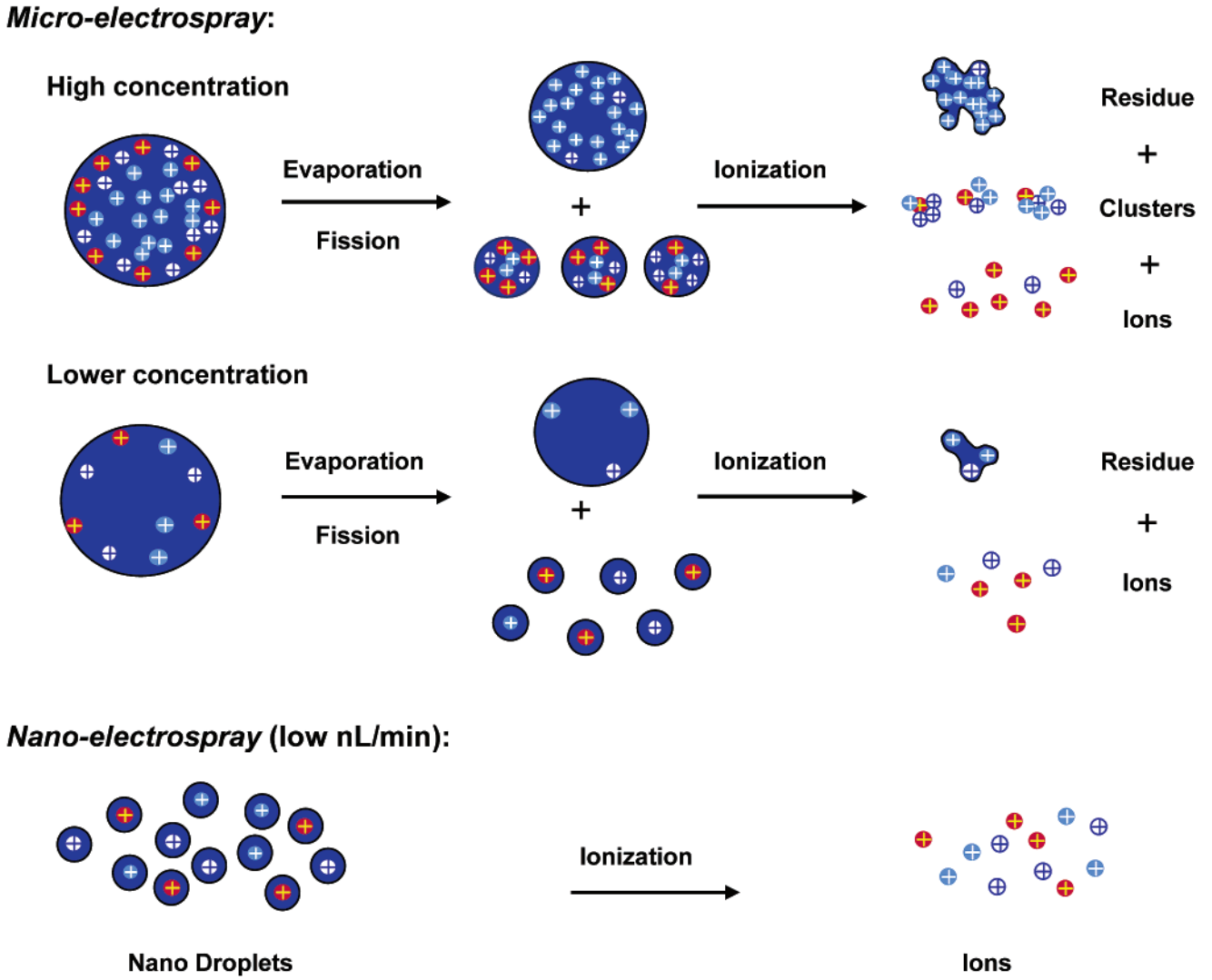


**FIGURE 2.** Simplified illustration showing concentration and flow rate effects on the ESI process. For larger flow rates, which produce larger droplets (Table 1), analyte surface activity, concentration, and competition from other species can affect overall ionization efficiency, the extent of ionization "suppression", and quantitation. At sufficiently low flow rates and analyte concentrations, each droplet contains on average less than one analyte molecule, ionization efficiency is 100%, and suppression/matrix effects are eliminated.

based upon droplet size and charge, as well as a chemical separation process whereby surface active compounds become enriched in the smaller droplets.[17] Larger flow rates result in greater compound-to-compound variations due to the effective competition for both charge and proximity to the droplet surface.[3,16] Thermodynamic constraints (e.g., relative proton affinities) and chemical properties, primarily surface activity, determine the "winners" (Figure 2, top). However, even at intermediate flow rates, ESI efficiencies often become more uniform and efficient at lower concentrations (Figure 2, middle), as illustrated by the spectra in Figure 3.

At low nanoliter per minute flow rates, biases recede as ionization efficiencies approach 100% (Figure 2, bottom). *If ions compete effectively with other solvent species for excess charge, then ionization suppression and matrix effects disappear*! Thus, nanoESI can be used to effectively study highly hydrophilic compound classes (e.g., oligosaccharides) that are conventionally problematic for ESI-MS due to low surface activity.[18,19] The flow rate at which ionization efficiencies approach 100% can be abrupt[19] and also depends on concentration; sufficiently high analyte concentrations can result in increasing contributions of analyte clusters (if their $m/z$ is detectable) and reappearance of bias effects (Figure 4).

## Nano-Flow-Rate Separations with ESI-MS

NanoESI allows samples as small as 1 $\mu$L to be analyzed for ~30 min, providing time for tuning, optimization, extended signal averaging, multistage MS analyses, etc. If the same sample is subjected to a high-quality separation, providing 10-s-wide peaks, then a ~200-fold effective concentration for individual components can be obtained. This results in not only superior detection limits compared to extended signal averaging with nanoESI but also greatly reduced mass spectral complexity at any point due to separation from other mixture components, as well as background species, contaminants, etc. (often lumped together as "chemical noise").

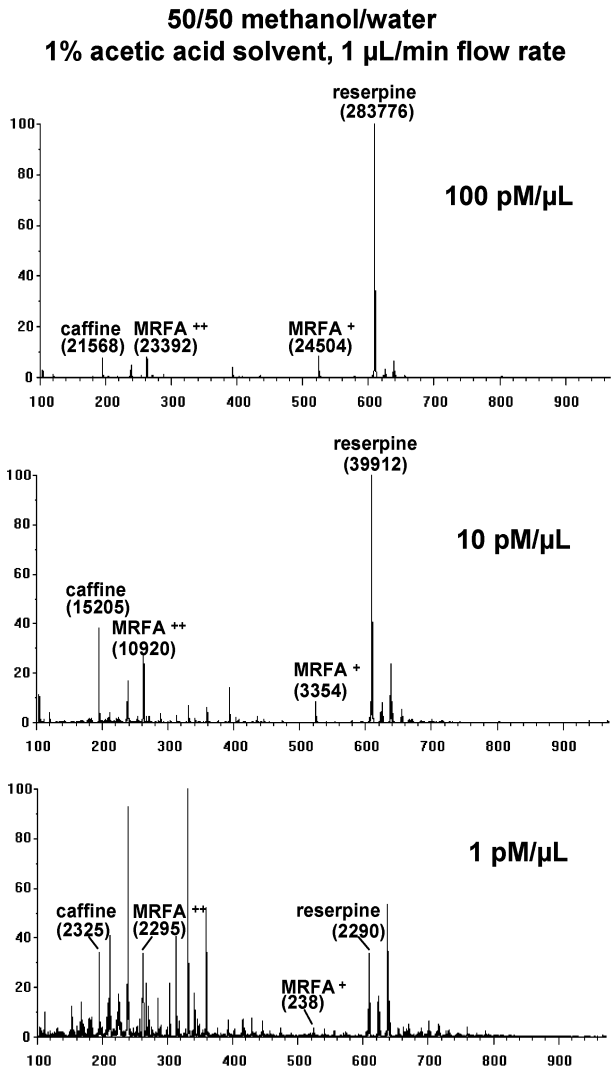


**FIGURE 3.** Mass spectra for a three-component mixture at three concentrations. At the highest concentration (top), reserpine displays greater intensity than other components, but peak intensities become nearly equivalent at the lowest concentration (bottom). As electrospray flow rate is decreased, ionization competition/suppression is avoided at increasingly higher concentrations (Figure 2).

The challenge is to develop separations at low nanoliter per minute flow rates that can (1) handle typical sample volumes, (2) provide high-efficiency (peak capacity) separations, and (3) be effectively coupled to ESI-MS.

We have explored both CE[10] and reversed-phase gradient capillary and nanoscale liquid chromatography (cLC and nanoLC)[20,21] to address these issues. We currently focus on nanoLC since the range of peptides that can be addressed and the separation quality (e.g., peak capacities) presently achievable with ESI-compatible buffer systems are better than those presently obtained with CE.

## High-Efficiency Nano-Flow LC with ESI-MS

The easiest implementation of LC separations with nanoESI involves splitting the flow from a conventional separation. For example, a 150 $\mu$m i.d. capillary packed with a 2−3 $\mu$m diameter particle stationary phase would have a flow rate of ~1.5 $\mu$L/min. A split ratio of ~1:100 would provide a 15 nL/min flow rate, but this approach would also effectively waste 99% of the sample.

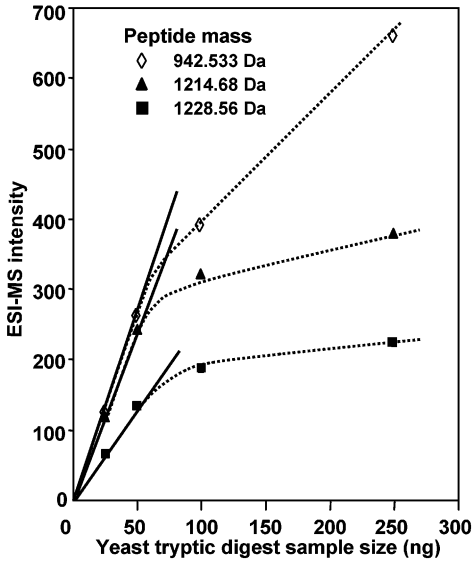


**FIGURE 4.** ESI-MS peak intensities vs total sample size for three high-abundance peptides in a tryptic digest of a yeast lysate separated using a 30 $\mu$m i.d. packed capillary (~80 nL/min flow rate). For sample sizes below a given level, MS peak intensities (or peak areas) increase linearly with sample size; above this level, suppression effects are evident.[21]

Obtaining high-quality LC separations at nano-flow rates presents challenges, the first of which involves introducing the sample to the column. The resistance inherent with narrower and longer packed capillaries extends sample injection times. For example, it takes ~500 min to load a 10 $\mu$L sample into a 90 cm × 15 $\mu$m i.d. column using the highest practical pressure. To shorten injection times, we developed a readily automated arrangement that quickly loads samples on a short precolumn having ~3-fold greater i.d. than the analytical capillary. With use of a 4 cm long, 50 $\mu$m i.d. precolumn (with an 86 cm long, 15 $\mu$m i.d. analytical column), a 10 $\mu$L sample can be loaded in ~1.5 min.[22]

Another challenge is efficient packing of long, small i.d. columns; however, once made, these columns function robustly for extended periods (typically hundreds of analyses over many months).[23] While availability of smaller and more uniform particles would improve packing, promising alternatives include open tubular columns, where the stationary phase is coated on the inside capillary wall,[24] or monolithic columns where the stationary phase support is polymerized in situ.[25]

The smallest i.d. LC columns used to date have 15 $\mu$m i.d.; an ~85 cm long column that provides a flow rate of ~20 nL/min at optimal linear separation velocity requires ~10 000 psi. With these columns, ESI efficiency is expected to be as much as 100-fold greater than that with 150 $\mu$m i.d. columns, and MS peak intensities (or LC peak areas) generally increase linearly with abundance, becoming nonlinear above a certain threshold (Figure 4).[21] However, nonlinear response for some lower abundance peptides can still occur, for example, due to selective losses to surfaces.

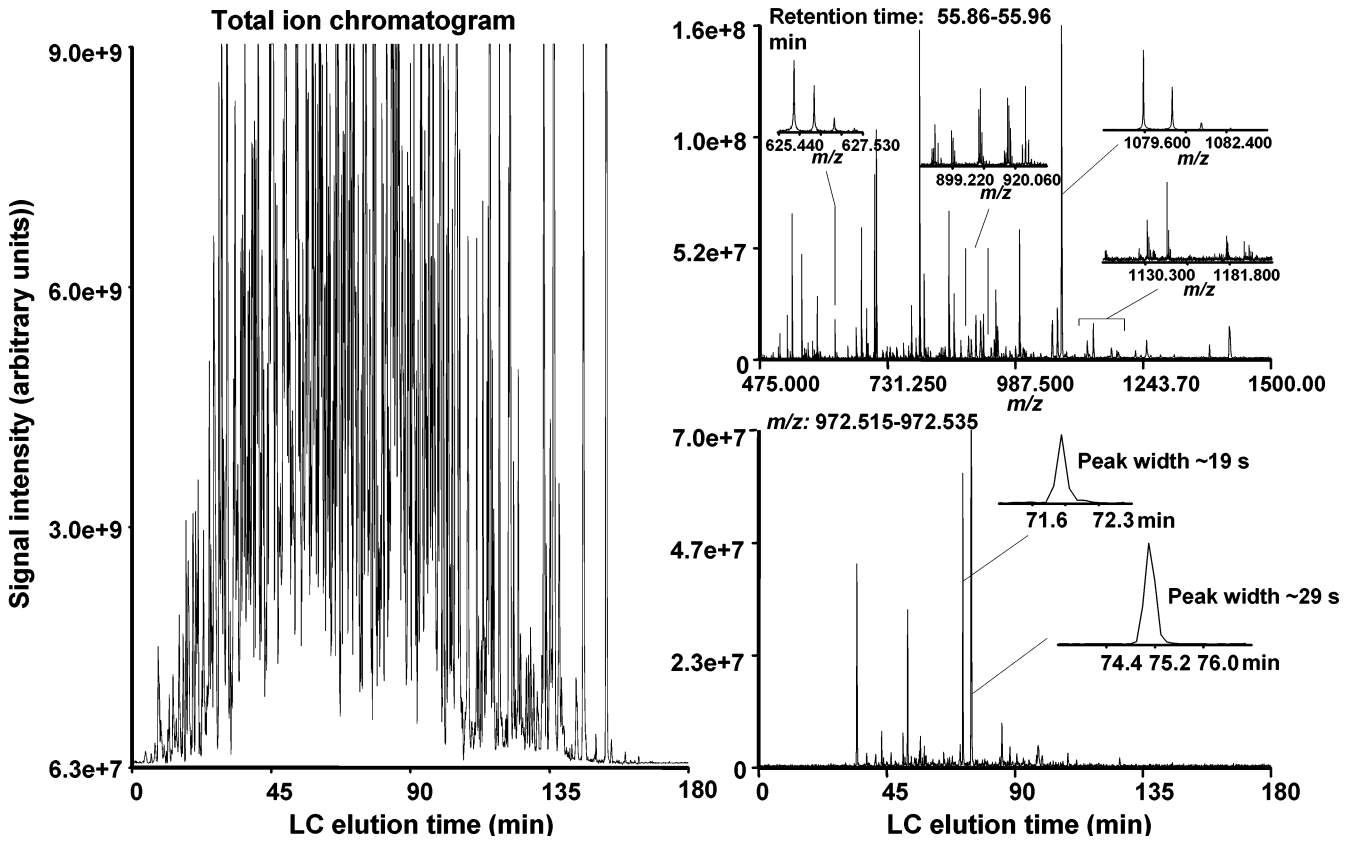


**FIGURE 5.** Gradient reversed-phase capillary LC−FTICR chromatogram for a tryptic digest of a yeast lysate of soluble proteins[26] (left) in which ~100 000 different putative peptides were detected. A narrow *m/z* range chromatogram (right, bottom) shows peak widths for two species. Peaks are generally wider for more abundant species, expanding the effective dynamic range of measurements. A portion of one spectrum (right, top) illustrates the high density of data obtained in just one spectrum during this separation.

The 15 $\mu$m i.d. columns provide peak capacities of ~1000.[21] While total peak capacity can be further increased by adding more separation stages, a single separation stage with comparable peak capacity is preferable because it enhances throughput and minimizes redundant detection of components in "adjacent" first-dimension fractions as well as losses of irreversibly retained compounds from the first-dimension fractions.

Separation quality largely determines overall dynamic range and the coverage of proteomics analyses. In one case, the number of peptides detected with LC−Fourier transform ion cyclotron resonance (FTICR) increased ~3-fold by improving the separation peak capacities from ~$10^2$ to ~$10^3$.[20] Similarly, improving LC peak capacities from ~550 to ~1000 doubled the number of peptides identified with tandem mass spectrometry (MS/MS).[22]

## Ion Utilization and Detection Sensitivity for ESI-MS

The near-perfect ionization efficiency provided by nanoLC−ESI can be fully exploited only if matched by MS performance. Early ESI-MS instruments suffered due to inefficient ion transmission to the detector. Generally the greatest ion losses are in the higher pressure regions. Collisional focusing at pressures of $<10^{-2}$ Torr in RF ion guides[27] can provide near 100% transmission efficiency. A well-designed mass spectrometer can have overall efficiencies of ion transmission and detection in lower pressure regions that can significantly exceed 10%. However, conventional ion optics are less effective for ion transfer from the first vacuum stage (typically at a pressure of 1−5 Torr) to lower pressure regions.

To minimize these losses, we developed the electrodynamic ion funnel.[28] The ion funnel uses a series of progressively smaller diameter ring electrodes to which RF potentials are applied with opposite phases to adjacent elements to confine ions. A separate DC field is applied to drive ions "down the throat" of the funnel, and ion transmission efficiency through the ion funnel is essentially 100% over a wide $m/z$ range.[29,30] We further refined the ESI−ion funnel interface to incorporate multiple inlet channels,[31] a jet disrupter that allows higher pressure operation, [32] and a dual ion funnel variation, including a separately controllable channel for calibrant introduction.[33]

In conjunction with nano-flow ESI, it is now possible to achieve high overall efficiencies for ion formation and transmission to the MS analyzer. How efficiently ions are utilized in analyses is then dictated by the type of instrument and operational details. Belov et al. showed overall ion utilization (from ionization through detection) of 7−10%, providing low zeptomole detection limits for proteins.[34]

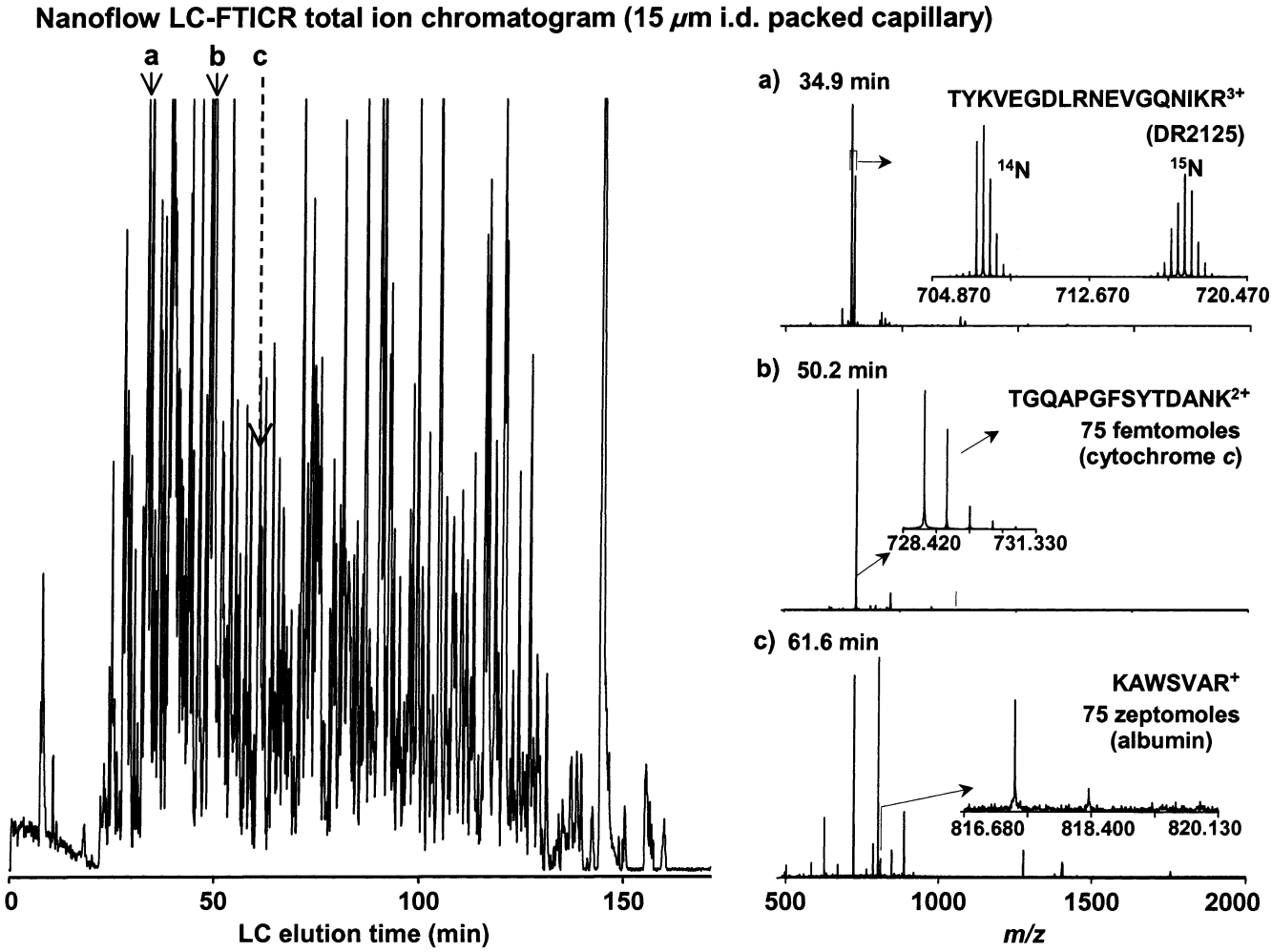


**FIGURE 6.** Illustration depicting the range of relative protein abundances detectable using low nano-flow LC−FTICR for analysis of 5 ng of $^{14}N/^{15}N$-labeled *D. radiodurans* tryptic digest sample spiked with 75 fmol of cytochrome *c* and 75 zmol of bovine serum albumin. Three spectra (right) show detection of a typical tryptic peptide from *D. radiodurans* in both labeled forms and two peptides from the spiked proteins.

## ESI−Fourier Transform Ion Cyclotron Resonance (FTICR)−MS

FTICR excels in resolution and accuracy of mass measurements.[35] Sensitivity depends on the efficiency of ion transfer to the FTICR cell, as well as trapping and detection efficiency. Important characteristics of FTICR detection are as follows: ~50 charges are needed to provide a S/N ≈ 3,[36] the maximum trap capacity due to the onset of deleterious space charge effects is $\sim 10^6-10^7$ charges (depending primarily upon magnetic field strength and trap volume), and each spectrum requires ~1 s to acquire.

Most instruments now invoke the intermediate step of ion accumulation in an "external" multipole ion trap followed by transfer to the FTICR trap in the high magnetic field.[37] Controlling the ion trap population is important for realizing the widest possible MS dynamic range. We developed "automated gain control" (AGC) to extend accumulation periods when the rate of ion formation is low (between the elution of major peaks in a separation) and thus provide an overall dynamic range exceeding that obtainable in any single spectrum.[38,39] AGC also helps avoid excessive ion populations that degrade mass measurement accuracy.

Over the past decade, we have developed and refined several ESI−FTICR instruments to optimize sensitivity and other aspects of performance for bioanalytical applications (Figure 5). At present, species differing by at least 3000 in peak intensity can be observed in a single spectrum, and *at least* 6 orders of magnitude differences in relative protein abundances can be characterized with LC/FTICR (Figure 6). A detection limit of 10 zmol (i.e., ~6000 molecules) was estimated for tryptic peptides from albumin, and a peptide concentration detection limit of ~250 aM was determined on the basis of amenable sample volumes.[23] A *Deinococcus radiodurans* proteome sample size of only 0.5 pg allowed identification of the more abundant proteins that accounted for ~0.2−2% (w/w) of the total protein content. On the basis of these results, sufficient sensitivity exists to cover a range of $>10^3$ relative protein abundances for the more abundant proteins from a single mammalian cell *if* compatible sample handing capabilities are available. The challenge of effectively processing such small samples most likely will be met by the use of yet to be developed microfabricated devices.

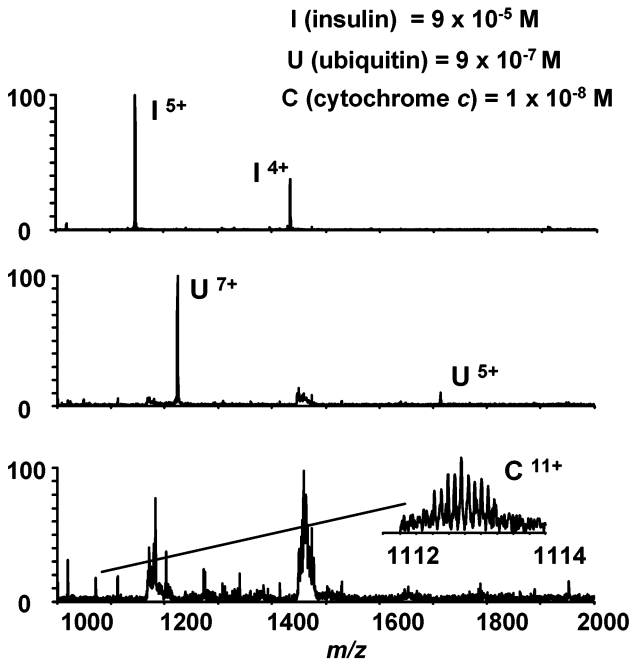


**FIGURE 7.** Demonstration of the increased dynamic range afforded by applying broadband QE to remove high-abundance species and allow the FTICR cell to be filled with lower-abundance species. The "normal" spectrum (top) provides the information needed for removal of the major insulin peaks in the next spectrum (middle). The process was then repeated, resulting in ejection of ubiquitin peaks, which allowed the lowest-abundance protein in the bottom spectrum to be detected (an $\sim 10^2$ gain in detection range).

## The Dynamic Range Challenge

With AGC, the greatest sensitivity is obtained only for portions of separations having low signal intensities where accumulation times are longest. Highly abundant species preclude detection in the same spectrum of otherwise detectable low-abundance species. Since it is possible to transmit $>10^8$ charge/s, the maximum ion transmission rates from an ESI source can greatly exceed what FTICR can handle, effectively wasting useful signal.

An approach for achieving higher dynamic range measurements is to fill the FTICR trap with a desired subset of ions. Selective ion accumulation (SIA) using quadrupole excitation (QE) methods allows the FTICR cell to be "filled" with specific species from complex mixtures and is well suited for species that can be targeted in advance. To identify low-level species for which the $m/z$ is *not* known in advance, we extended and generalized the SIA approach by using rapidly synthesized "colored noise" QE waveforms to enable automated dynamic range expansion by magnetron ejection of species *not* subjected to QE.[40] This automated process removes high-intensity species from the *next* mass spectrum (Figure 7). A disadvantage of this technique was the need to introduce a gas for magnetron ejection, which resulted in slower spectrum acquisition and reduced compatibility with separations.

To overcome this limitation, we developed dynamic range enhancement applied to mass spectrometry (DREAMS),[41] where a normal mass spectrum is followed by a spectrum in which the most abundant ions detected in the previous spectrum are removed in a quadrupole device outside the magnetic field, avoiding gas introduction to the FTICR trap. With this approach, overall dynamic range was extended >10-fold (Figure 8). In one application using DREAMS, we found the number of peptides detected in a proteome analysis increased by about 35%.[41] In another application involving a mixture of natural isotopic abundance and $^{15}$N-labeled *D. radiodurans* proteins, the number of identified peptides detected in both natural and $^{15}$N-labeled labeled forms, for use in quantitation, increased by ~50%. Additionally, the total of 1244 proteins identified (~40% of the predicted proteome), included 279 proteins detected only in the DREAMS set of spectra.[42]

## An Accurate Mass and Time (AMT) Tag Strategy for High-Throughput Proteomics

Currently, the most effective approaches for protein characterization by mass spectrometry involve digesting the protein to smaller peptide fragments, since nearly all proteins yield sets of distinctive peptides. Protein identification typically involves selecting peptides one-at-a-time in the first stage MS for collisional dissociation. The fragments are analyzed by a second MS stage to obtain sufficient sequence-related information for peptide identification. A key point is that when many peptides are present simultaneously after LC separation, only a subset of the peptides can generally be identified by MS/MS.[43] This "too many peaks, too little time" under-sampling problem can be addressed by better (and longer) separations, at the expense of lower throughput and increased sample consumption, and constitutes a major throughput bottleneck.

To address this problem, we developed an approach that utilizes high mass measurement accuracy and separations (elution times). A multidimensional LC separations strategy followed by MS/MS is used to identify peptides, essentially the "shotgun" proteomics approach developed by Yates and co-workers.[44] These experiments serve to identify peptides and show where they elute in a separation and subsequently to define AMT peptide tags after confirmation that the predicted mass is observed to high accuracy at the same normalized elution time. Thus, AMT tags correspond to "protein markers" and enable greater sensitivity and throughput since it is possible to identify up to hundreds of peptides in each spectrum in all subsequent proteome analyses. The AMT tag strategy facilitates quantitative measurements of relative abundances using stable-isotope labeling. Both the accurate mass information from FTICR and the use of elution time information increase the confidence in protein identifications.[45]

The AMT tag strategy was initially applied to the microorganism *D. radiodurans*, providing confident identification of 1910 predicted proteins that covered ~61% of the expected gene products from annotated open reading frames in the sequenced genome and included 715 proteins previously annotated as either hypothetical or con-

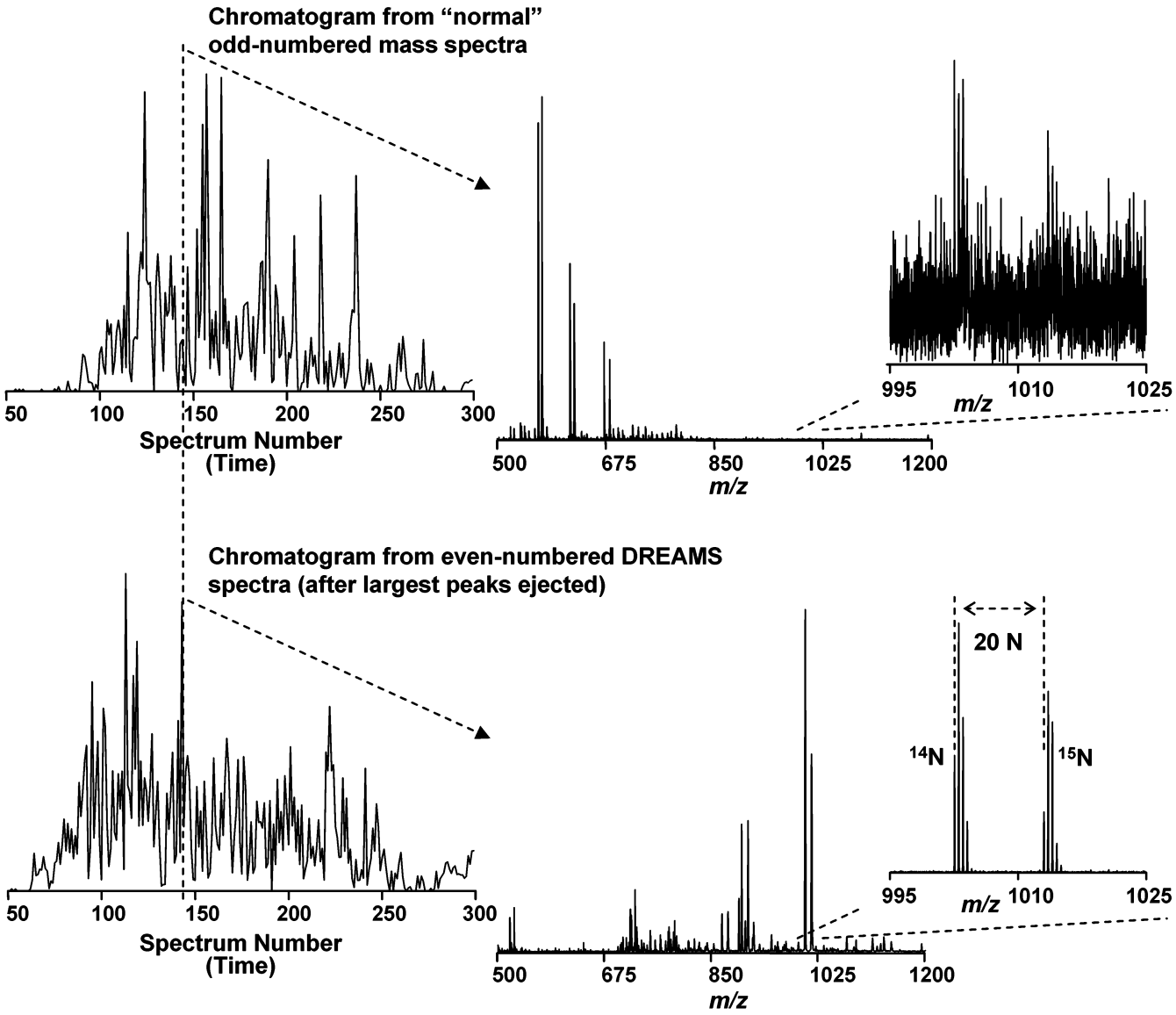


**FIGURE 8.** Partial chromatograms and examples of typical "normal" and DREAMS spectra from a capillary LC−FTICR analysis of peptides from a tryptic digest of a mixture of natural isotopic abundance and $^{15}$N-labeled mouse B16 proteins: (top left) partial chromatogram reconstructed from the normal FTICR mass spectra; (bottom left) corresponding chromatogram from the DREAMS spectra for which high relative abundance species were ejected, allowing longer ion accumulation. The mass spectra (center) show the effective ejection of the major species in the top spectrum compared to the one shown on the bottom. The detail (right) shows a large gain in sensitivity and S/N for a peptide pair providing a basis for quantitative comparison of protein abundances in the two cell cultures.

served hypothetical.[46] AMT tags were then used to study the proteomes of *D. radiodurans* cultured under 15 conditions.

The AMT tag approach continues to be refined and is presently being extended to mammalian proteomes. This strategy is also applicable to modified peptides, intact proteins, and other compounds (e.g., metabolites) and likely provides the greatest achievable throughput and sensitivity for MS characterization of complex mixtures.

## Additional Challenges and Opportunities

Advances in instrumentation and computational technologies are propelling broader application of MS in proteomics research. It is now possible to study thousands of proteins within a single experiment. This capability potentially allows cellular pathways and networks, as well as how they affect one another, to be elaborated or characterized in hours instead of months or years.

The basis now exists for proteomic studies of samples as small as a single mammalian cell. We believe that there is no fundamental constraint in approaching 100% efficiency for the overall creation and analysis of ions by nanoLC−ESI-MS. Currently, overall efficiency is ~10%, within a factor of 10 of this goal, but significant challenges remain. Effective ESI emitters for small orifice dimensions (~1 $\mu$m) must be fabricated to provide for even lower ESI flow rates. Some losses, particularly at the mass spectrometer's ESI inlet, remain to be addressed. Detector efficiency/sensitivity needs to be improved (e.g., microchannel plate detectors used in TOF instrumentation are

only ~75% efficient), although the measurement of single protein ions by FTICR has already been demonstrated.[36] Achieving 100% efficiency would open qualitatively new opportunities, such as high-speed DNA sequencing based upon the mass measurement of nucleotides progressively released by exonuclease processing of a long DNA strand immobilized in a liquid flow to a nanoESI emitter.

Finally, we note the qualitatively new opportunities afforded by the combined capabilities for highly sensitive proteome analyses that are fast enough to address large numbers of very small samples. One might involve making detailed three-dimensional mouse brain proteome "images" for the abundances of each of the array of detectable proteins. Corresponding gene expression images have already been reported.[47] The corresponding capability at the protein level, facilitated by the practical capability for making proteomics analyses of the ~500 small volume (~1 $\mu$L) tissue cubes (voxels) per mouse brain, will likely provide new insights into the biochemical basis of cognition and mouse models of disease states (e.g., Parkinson's disease).

*We thank the U.S. Department of Energy's Office of Biological and Environmental Research, the Environmental Molecular Sciences Laboratory for use of instrumentation, and the National Institutes of Health (Grants CA81654 and RR18522) for support of portions of this work.*

## References

(1) Fenn, J. B.; Mann, M.; Meng, C. K.; Wong, S. F.; Whitehouse, C. M. Electrospray Ionization-Principles and Practice. *Mass Spectrom. Rev.* **1990**, *9*, 37−70.
(2) Hillenkamp, F.; Karas, M.; Beavis, R. C.; Chait, B. T. Matrix-Assisted Laser Desorption Ionization Mass-Spectrometry of Biopolymers. *Anal. Chem.* **1991**, *63*, 1193A−1202A.
(3) Cech, N. B.; Enke, C. G. Practical Implications of Some Recent Studies in electrospray Ionization Fundamentals. *Mass Spectrom. Rev.* **2001**, *20*, 362−387.
(4) Tang, K.; Gomez, A. On the Structure of an Electrostatic Spray of Monodisperse Droplets. *Phys Fluids* **1994**, *6*, 2317−2332.
(5) Gomez, A.; Tang, K. Charge and Fission of Droplets in Electrostatic Sprays. *Phys. Fluids* **1994**, *6*, 404−414.
(6) Fernandez de la Mora, J. Electrospray Ionization of Large Multiply Charged Species Proceeds via Dole's Charged Residue Mechanism. *Anal. Chim. Acta* **2000**, *406*, 93−104.
(7) Felitsyn, N.; Peschke, M.; Kebarle, P. Origin and Number of Charges Observed on Multiply-protonated Native Proteins Produced by ESI. *Int. J. Mass Spectrom.* **2002**, *219*, 39−62.
(8) Light-Wahl, K. J.; Schwartz, B. L.; Smith, R. D. Observation of the Noncovalent Quaternary Associations of Proteins by Electrospray Ionization Mass Spectrometry. *J. Am. Chem. Soc.* **1994**, *116*, 5271−5278.
(9) Bruins, A. Mass Spectrometry with Ion Sources Operating at Atmospheric Pressure. *Mass Spectrom. Rev.* **1991**, *10*, 53−77.
(10) Olivares, J. A.; Nguyen, N. T.; Yonker, C. R.; Smith, R. D. On-Line Mass Spectrometric Detection for Capillary Zone Electrophoresis. *Anal. Chem.* **1987**, *59*, 1230−1232.
(11) Wahl, J. H.; Goodlett, D. R.; Udseth, H. R.; Smith, R. D. Attomole Level Capillary Electrophoresis Mass-Spectrometric Protein-Analysis Using 5-$\mu$m-i.d. Capillaries. *Anal. Chem.* **1992**, *64*, 3194−3196.
(12) Smith, R. D.; Wahl, J. H.; Goodlett, D. R.; Hofstadler, S. A. Capillary Electrophoresis/Mass Spectrometry. *Anal. Chem.* **1993**, *65*, A574−A584.
(13) Gale, D. C.; Smith, R. D. Small Volume and Low Flow-Rate Electrospray Ionization Mass Spectrometry of Aqueous Samples. *Rapid Commun. Mass Spectrom.* **1993**, *7*, 1017−1021.
(14) Wilm, M. S.; Mann, M. Electrospray and Taylor-Cone Theory, Dole's Beam of Macromolecules at Last? *Int. J. Mass Spectrom. Ion Processes* **1994**, *136*, 167−180.
(15) Fernandez de la Mora, J.; Loscertales, I. The Current Emitted by Highly Conducting Taylor Cones. *J. Fluid Mech.* **1994**, 155−184.
(16) Tang, L.; Kebarle, P. Dependence of Ion Intensity in Electrospray Mass Spectrometry on the Concentration of the Analytes in the Electrosprayed Solution. *Anal. Chem.* **1993**, *65*, 3654−3668.
(17) Tang, K.; Smith, R. D. Physical/Chemical Separations in the Break-up of Highly Charged Droplets from Electrosprays. *J. Am. Soc. Mass Spectrom.* **2001**, *12*, 343−347.
(18) Wilm, M.; Mann, M. Analytical Properties of the Nanoelectrospray Ion Source. *Anal. Chem.* **1996**, *68*, 1−8.
(19) Schmidt, A.; Karas, M.; Dülcks, T. Effect of Different Solution Flow Rates on Analyte Ion Signals in Nano-ESI MS, or When Does ESI Turn into Nano-ESI? *J. Am. Soc. Mass Spectrom.* **2003**, *23*, 492−500.
(20) Shen, Y.; Zhao, R.; Belov, M. E.; Conrads, T. P.; Anderson, G. A.; Tang, K.; Pasa-Tolic, L.; Veenstra, T. D.; Lipton, M. S.; Smith, R. D. Packed Capillary Reversed-Phase Liquid Chromatography with High-Performance Electrospray Ionization Fourier Transform Ion Cyclotron Resonance Mass Spectrometry for Proteomics. *Anal. Chem.* **2001**, *73*, 1766−1775.
(21) Shen, Y.; Zhao, R.; Berger, S. J.; Anderson, G. A.; Rodriguez, N.; Smith, R. D. High-Efficiency Nanoscale Liquid Chromatography Coupled On-line with Mass Spectrometry using Nanoelectrospray Ionization for Proteomics. *Anal. Chem.* **2002**, *74*, 4235−4249.
(22) Shen, Y.; Moore, R. J.; Zhao, R.; Blonder, J.; Auberry, D. L.; Masselon, C.; Pasa-Tolic, L.; Hixson, K. K.; Auberry, K. J.; Smith, R. D. High-Efficiency On-Line Solid-Phase Extraction Coupling to 15−150-$\mu$m-i.d. Column Liquid Chromatography for Proteomic Analysis. *Anal. Chem.* **2003**, *75*, 3596−3605.
(23) Shen, Y.; Tolić, N.; Masselon, C.; Paša-Tolić, L.; Camp, D. G., II; Hixon, K. K.; Zhao, R.; Anderson, G. A.; Smith, R. D. Ultrasensitive Proteomics using High-Efficiency On-Line Micro-SPE−NanoLC−Nano ES1 MS and MS/MS. *Anal. Chem.* **2004**, *76*, 144−154.
(24) Tock, P. P. H.; Stegeman, G.; Peerboom, R.; Poppe, H.; Kraak, J. C.; Unger, K. K. The Application of Porous Silica Layers in Open Tubular Columns for Liquid-Chromatography. *Chromatographia* **1987**, *24*, 617−624.
(25) Ivanov, A. R.; Zang, L.; Karger, B. L. Low-Attomole Electrospray Ionization MS and MS/MS Analysis of Protein Tryptic Digests Using 20-$\mu$m-i.d. Polystyrene−Divinylbenezene Monolythic Capillary Columns. *Anal. Chem.* **2003**, *75*, 5306−5316.
(26) Shen, Y. F.; Tolić, N.; Zhao, R.; Paša-Tolić, L.; Li, L. J.; Berger, S. J.; Harkewicz, R.; Anderson, G. A.; Belov, M. E.; Smith, R. D. High-throughput proteomics using high efficiency multiple-capillary liquid chromatography with on-line high-performance ESI FTICR mass spectrometry. *Anal. Chem.* **2001**, *73* (13), 3011−3021.
(27) Thomson, B. A. Radio Frequency Quadrupole Ion Guides in Modern Mass Spectrometry. *Can. J. Chem.* **1998**, *76*, 499−505.
(28) Kim, T.; Tolmachev, A. V.; Harkewicz, R.; Prior, D. C.; Anderson, G. A.; Udseth, H. R.; Smith, R. D.; Bailey, T. H.; Rakov, S.; Futrell, J. H. Design and Implementation of a New Electrodynamic Ion Funnel. *Anal. Chem.* **2000**, *72*, 2247−2255.
(29) Belov, M. E.; Gorshkov, M. V.; Udseth, H. R.; Anderson, G. A.; Tolmachev, A. V.; Prior, D. C.; Harkewicz, R.; Smith, R. D. Initial Implementation of an Electrodynamic Ion Funnel with FTICR Mass Spectrometry. *J. Am. Soc. Mass Spectrom.* **2000**, *11*, 19−23.
(30) Shaffer, S. A.; Tolmachev, A.; Prior, D. C.; Anderson, G. A.; Udseth, H. R.; Smith, R. D. Characterization of a New Electrodynamic Ion Funnel Interface for Electrospray Ionization Mass Spectrometry. *Anal. Chem.* **1999**, *71*, 2957−2964.
(31) Kim, T.; Udseth, H. R.; Smith, R. D. Improved Ion Transmission from Atmospheric Pressure to High Vacuum using a Multi-Capillary Inlet and Electrodynamic Ion Funnel Interface. *Anal. Chem.* **2000**, *72*, 5014−5019.
(32) Kim, T.; Tang, K.; Udseth, H.; Smith, R. A Multi-Capillary Inlet Jet Disruption Electrodynamic Ion Funnel Interface for Improved Sensitivity Using Atmospheric Pressure Ion Sources. *Anal. Chem.* **2001**, *73*, 4162−4170.
(33) Tang, K.; Tolmachev, A. V.; Nikolaev, E.; Zhang, R.; Belov, M. E.; Udseth, H. R.; Smith, R. D. Independent Control of Ion Transmission in a Jet Disrupter Dual-Channel Ion Funnel Electrospray Ionization MS Interface. *Anal. Chem.* **2002**, *74*, 5431−5437.
(34) Belov, M. E.; Gorshkov, M. V.; Udseth, H. R.; Anderson, G. A.; Smith, R. D. Zeptomole-Sensitivity Electrospray Ionization−Fourier Transform Ion Cyclotron Resonance Mass Spectrometry of Proteins. *Anal. Chem.* **2000**, *72*, 2271−2279.
(35) Marshall, A. G.; Hendrickson, C. L.; Jackson, G. S. Fourier Transform Ion Cyclotron Resonance Mass Spectrometry: A Primer. *Mass Spectrom. Rev.* **1998**, *17*, 1−35.
(36) Bruce, J. E.; Anderson, G. A.; Udseth, H. R.; Smith, R. D. Large Molecule Characterization Based Upon Individual Ion Detection with Electrospray Ionization-FTICR Mass Spectrometry. *Anal. Chem.* **1998**, *70*, 519−525.

(37) Senko, M. W.; Hendrickson, C. L.; Emmett, M. R.; Shi, S. D. H.; Marshall, A. G. External Accumulation of Ions For Enhanced Electrospray Ionization Fourier Transform Ion Cyclotron Resonance Mass Spectrometry. *J. Am. Soc. Mass Spectrom.* **1997**, *8*, 970−976

(38) Belov, M. E.; Zhang, R.; Strittmatter, E. F.; Prior, D. C.; Tang, K.; Smith, R. D. Automated Gain Control and Internal Calibration with External Ion Accumulation Capillary LC-ESI-FTICR. *Anal. Chem.* **2003**, *75*, 4195−4205.

(39) Belov, M. E.; Rakov, V. S.; Goshe, M. B.; Anderson, G. A.; Smith, R. D. Initial Implementation of External Accumulation Liquid Chromatography/Electrospray Ionization Fourier Transform Ion Cyclotron Resonance Mass Spectrometry with Automated Gain Control. *Rapid Commun. Mass Spectrom.* **2003**, *17*, 627−636.

(40) Bruce, J. E.; Anderson, G. A.; Smith, R. D. Colored Noise Waveforms and Quadrupole Excitation for the Dynamic Range Expansion of Fourier Transform Ion Cyclotron Resonance Mass Spectrometry. *Anal. Chem.* **1996**, *68*, 534−541.

(41) Belov, M. E.; Anderson, G. A.; Angell, N. H.; Shen, Y.; Tolic, N.; Udseth, H. R.; Smith, R. D. Dynamic Range Expansion Applied to Mass Spectrometry Based on Data-Dependent Selective Ion Ejection in Capillary Liquid Chromatography Fourier Transform Ion Cyclotron Resonance for Enhanced Proteome Characterization. *Anal. Chem.* **2001**, *73*, 5052−5060.

(42) Pasa-Tolic, L.; Harkewicz, R.; Anderson, G. A.; Tolic, N.; Shen, Y.; Zhao, R.; Thrall, B.; Masselon, C.; Smith, R. D. Increased Proteome Coverage Based upon High Performance Separations and DREAMS FTICR Mass Spectrometry. *J. Am. Soc. Mass Spectrom.* **2002**, *13*, 954−963.

(43) Tabb, D. L.; MacCoss, M. J.; Wu, C. C.; Anderson, S. D.; Yates, J. R. Similarity Among Tandem Mass Spectra from Proteomic Experiments: Detection, Significance, and Utility. *Anal. Chem.* **2003**, *75*, 2470−2477.

(44) Washburn, M. P.; Wolters, D.; Yates, J. R. Large-scale Analysis of the Yeast Proteome by Multidimensional Protein Identification Technology. *Nat. Biotechnol.* **2001**, *19*, 242−247.

(45) Smith, R. D.; Anderson, G. A.; Lipton, M. S.; Pasa-Tolic, L.; Shen, Y.; Conrads, T. P.; Veenstra, T. D.; Udseth, H. R. An Accurate Mass Tag Strategy for Quantitative and High Throughput Proteome Measurements. *Proteomics* **2002**, *2*, 513−523.

(46) Lipton, M. S.; Pasa-Tolic, L.; Anderson, G. A.; Anderson, D. J.; Auberry, D. L.; Battista, J. R.; Daly, M. J.; Fredrickson, J.; Hixson, K. K.; Kostandarithes, H.; Masselon, C.; Markillie, L. M.; Moore, R.; Romine, M. F.; Shen, Y.; Strittmatter, E.; Tolic, N.; Udseth, H. R.; Venkateswaran, A.; Wong, K. K.; Zhao, R.; Smith, R. D. Global Analysis of the *Deinococcus radiodurans* R1 Proteome by using Accurate Mass Tags. *Proc. Natl. Acad. Sci. U.S.A.* **2002**, *99*, 11049−11054.

(47) Brown, V. M.; Ossadtchi, A.; Khan, A. H.; Yee, S.; Lacan, G.; Melega, W. P.; Cherry, S. R.; Leahy, R. M.; Smith, D. J. Multiplex Three-dimensional Brain Gene Expression Mapping in a Mouse Model of Parkinson's Disease. *Genome Res.* **2002**, *12*, 868−884.

AR0301330